

RESEARCH ARTICLE

Jiang et al.: SPDEF's role in PAAD progression

SPDEF drives pancreatic adenocarcinoma progression via transcriptional upregulation of S100A16 and activation of the PI3K/AKT signaling pathway

Hang Jiang^{1#}, Zhiqian Xue^{1#}, Liping Zhao^{1#}, Boyuan Wang², Chenfei Wang^{3*}, Haihan Song^{1,4,5*}, Jianjun Sun^{1*}

1. Department of Hepatobiliary and Pancreatic Surgery, The Third People's Hospital of Yunnan Province, Kunming, Yunnan, China.
2. Shanghai Qibao Dwight High School, Shanghai, China.
3. Department of Emergency, Renji Hospital, School of Medicine, Shanghai Jiao Tong University, Shanghai, China.
4. Department of Immunology, DICAT Biomedical Computation Centre, Vancouver, BC, Canada.
5. Central Lab, Shanghai Key Laboratory of Pathogenic Fungi Medical Testing, Shanghai Pudong New Area People's Hospital, Shanghai, China.

***Corresponding authors:** Jianjun Sun; E-mail: 1468844024@qq.com; Chenfei Wang;

E-mail: drwangcf@126.com; Haihan Song; E-mail: haihansongsh@163.com.

#These authors contributed equally to this manuscript.

DOI: <https://doi.org/10.17305/bb.2024.10346>

Conflicts of interest: Authors declare no conflicts of interest.

Funding: Xing Dian Talent Support Program (2023MY007); Medical Discipline Construction Project of Pudong Health Committee of Shanghai (PWYts2021-18)

Data availability: Information on the accessibility of data and materials provided by the authors is available in the supplementary material.

Submitted: 5 February 2024 / **Accepted:** 15 March 2024 / **Published:** 23 March 2024

ABSTRACT

Pancreatic adenocarcinoma (PAAD) is a notably aggressive malignancy with limited treatment options and an unfavorable prognosis for patients. We aimed to investigate molecular mechanisms by which Sam's pointed domain-containing ETS transcription factor (SPDEF) exerts effects on PAAD progression. We analyzed differentially expressed genes (DEGs) and their integration with ETS family members using the The Cancer Genome Atlas (TCGA) database, hence identifying *SPDEF* as a core gene in PAAD. Kaplan-Meier survival analysis confirmed SPDEF's prognostic potential. In vitro experiments validated the association with cell proliferation and apoptosis, affecting pancreatic cancer cell dynamics. We detected increased SPDEF expression in PAAD tumor samples. Our in vitro studies revealed that SPDEF regulates mRNA and protein expression levels, and significantly affects cell proliferation. Moreover, SPDEF was associated with reduced apoptosis and enhanced cell migration and invasion. In-depth analysis of SPDEF-targeted genes revealed four crucial genes for advanced prognostic model, among which *S100A16* was significantly correlated with SPDEF. Mechanistic analysis showed that SPDEF enhances the transcription of *S100A16*, which in turn enhances PAAD cell migration, proliferation, and invasion by activating the PI3K/AKT signaling pathway. Our study revealed the critical role of SPDEF in promoting PAAD by upregulating *S100A16* transcription and stimulating the PI3K/AKT signaling pathway. This knowledge deepened our understanding of pancreatic cancer's molecular progression and unveiled potential therapeutic strategies targeting SPDEF-driven pathways.

Keywords: Pancreatic adenocarcinoma (PAAD), Sam's pointed domain-containing
ETS transcription factor (SPDEF), S100A16, PI3K/AKT signaling pathway

INTRODUCTION

The rapid increase in the global prevalence of pancreatic adenocarcinoma (PAAD) underscores the critical importance of early detection and timely intervention (1, 2). Its insidious nature and the absence of distinctive early symptoms often lead to delayed diagnosis, at which point the disease has frequently advanced to an inoperable stage (3, 4). This late detection, combined with the aggressive progression of the cancer, considerably complicates treatment, and reduces the likelihood of a positive outcome for the patient. Furthermore, the inherent resistance of PAAD to several conventional treatments means that even if diagnosed early, the treatment effectiveness may still be limited (5). The PAAD's genetic heterogeneity indicates that tailored treatment regimens could be more efficacious than generic strategies (6, 7). Advancements in personalized medicine and genomic profiling offer promising avenues in this realm. Recognizing the specific genetic aberrations and molecular mechanisms of individual tumors may enable clinicians to design more precise and effective therapeutic interventions.

The PI3K/AKT signaling pathway, pivotal for cellular homeostasis and growth, becomes detrimental when dysregulated, contributing to various diseases, notably cancer (8, 9). Its significance in PAAD is emphasized by its complex web of signaling cascades, feedback mechanisms, and interactions with other pathways that jointly determine the trajectory of cancer cells (10, 11). Aberrant activation of the PI3K/AKT pathway provides a proliferative edge to pancreatic tumor cells (12). This

overactivation propels unchecked cell proliferation, circumvents apoptotic processes, and stimulates angiogenesis, all crucial for tumor sustenance (13, 14). Furthermore, this signaling pathway can promote metastasis, a primary factor in PAAD fatalities (15). Recent studies by Stanciu et al. and Li et al. have enriched our understanding of this pathway's intricacies in pancreatic cancer. Stanciu et al. emphasized the role of cytokines, chemokines, and growth factors in activating PI3K/AKT/mTOR signaling, shedding light on external factors modulating pancreatic tumor intracellular mechanisms (16). Conversely, Li et al. unveil therapeutic prospects by showcasing how scoparone, a natural compound, may counteract pancreatic cancer by targeting this pathway (17). Therefore, delving into the nuances of the PI3K/AKT pathway, it offers insights into pancreatic cancer mechanisms and promises targeted therapeutic avenues.

The Sam's pointed domain-containing ETS transcription factor (SPDEF), while implicated in various cellular processes, has not been extensively explored in the context of PAAD. Unveiling the role of novel molecules, such as SPDEF, in the complex molecular landscape of pancreatic cancer may be pivotal for crafting innovative therapeutic avenues. A key focus of our investigation is the relationship between SPDEF and S100A16, its purported downstream effector. Elucidation of this regulatory axis may provide insight into novel molecular mechanisms that may influence PAAD aggressiveness. S100A16, a member of the S100 protein family known for calcium binding and cellular signaling, may play a nuanced role in tumorigenesis, especially in conjunction with SPDEF (18, 19). Furthermore, given the

significance of the PI3K/AKT signaling pathway in various cancers, the potential interplay between SPDEF, S100A16, and this pathway is of considerable interest. Such interactions could offer profound insights into novel avenues of tumor progression and therapeutic resistance. As we investigate further into the role of SPDEF, its potential as a prognostic marker could also emerge, providing valuable insights for predicting disease trajectories and guiding treatment decisions in malignancies like PAAD.

In summary, this research aspired to traverse the complexities of the SPDEF-S100A16-PI3K/AKT axis in the context of PAAD. By piecing together this molecular puzzle, we hope to carve out a clearer picture of PAAD's molecular landscape, offering avenues for targeted treatments and, more importantly, hope for patients diagnosed with this formidable malignancy.

MATERIALS AND METHODS

Differential gene expression and survival analysis in PAAD

The 179 PAAD samples and 4 normal samples were obtained from The Cancer Genome Atlas (TCGA) database (<https://tcga-data.nci.nih.gov/tcga/>). By using the "ggplot2" package in R, differential gene expression analysis was done on the TCGA PAAD dataset. Genes were filtered based on fold change (FC) criteria: $FC > 2$ or $FC < 0.5$, and $P < 0.05$ was used as the significance criterion. The distribution of differentially expressed genes (DEGs) was shown using a volcano plot. The "VennDiagram" package was employed to identify genes that overlapped between the DEGs and the ETS family of genes. The intersection of these gene sets was visualized using Venn diagrams to determine shared candidates for further investigation. The Kaplan-Meier (KM) survival analysis was used to evaluate the prognostic significance of the hub *SPDEF* gene in relation to overall survival (OS) and recurrence-free survival (RFS) for patients with pancreatic cancer. The appropriate R packages were used to calculate the survival probabilities and log-rank P -values. The relationship between *SPDEF* expression and patient outcomes was assessed by contrasting the high and low-expression groups.

Expression analysis and staging evaluation of *SPDEF* in PAAD

SPDEF expression analysis was performed using the PAAD dataset from the TCGA database. Raw expression data was obtained, and the R Studio was utilized for data processing and visualization. By using the "ggplot2" package in R, boxplots showing the distribution of *SPDEF* expression in PAAD samples were visualized and *SPDEF*

expression levels evaluated. The relationship between *SPDEF* expression and various pancreatic cancer stages was assessed using the gene expression profiling interactive analysis (GEPIA; <http://gepia.cancer-pku.cn/>) database. Genotype Tissue Expression (GTEx) and TCGA studies have both produced gene expression data, which is thoroughly analyzed by GEPIA. *SPDEF* expression at different tumor stages was assessed using the "Stage Map" function available in the GEPIA web interface. The association of *SPDEF* expression with M (metastasis) and N (lymph node) stages was assessed based on clinical data and medical imaging records. Information on metastases and lymph node involvement was collected from clinical reports, imaging studies, and pathological examinations of patients with PAAD. This multifaceted approach involving TCGA, GEPIA, and clinical data enabled a comprehensive analysis of *SPDEF* expression patterns and their potential association with the PAAD tumor stage.

hTFtarget database

The human transcription factor target gene (hTFtarget, <http://bioinfo.life.hust.edu.cn/hTFtarget/>) database is specifically designed to predict transcription factor target genes and delineate their regulatory interactions. Hence, to discern *SPDEF* target genes, we employed the hTFtarget database. This predicted genes potentially regulated by *SPDEF*. Subsequently, an intersection analysis was conducted between these predicted genes and the upregulated DEGs (**Supplementary table 1**). This approach provided a more comprehensive understanding of the downstream *SPDEF*-associated regulatory network in the milieu of PAAD.

Prognostic analysis of *SPDEF*-related genes in PAAD

Prediction of *SPDEF* target genes was performed using the hTFtarget database, which integrates transcription factor-target interactions. Thirty genes with significantly altered expression in pancreatic cancer were found when upregulated DEGs and *SPDEF*-predicted target genes were combined together. This subset of genes was subjected to least absolute shrinkage and selection operator (LASSO) regression analysis in order to create a forecasting model. The optimal lambda value ($\lambda_{\min} = 0.0722$) was determined by LASSO regression analysis. This approach facilitates the identification of key genes for subsequent prognostic modeling. To develop a prognostic risk model, based on the expression levels of four significant genes discovered using this method, a risk score was created. The risk score was calculated based on the expression levels of four important genes obtained from LASSO analysis. The risk score formula is as follows:

$$\begin{aligned} \text{risk score} = & 0.1266 \times \text{MYEOV} + 0.1765 \times \text{ECT2} + 0.0621 \times \text{MMP28} \\ & + 0.0291 \times \text{S100A16} \end{aligned}$$

The TCGA database containing pancreatic cancer tumor samples was used for risk score calculation. Based on the median risk score, the samples were then split into high- and low-risk groups. The performance of the generated risk models was evaluated by survival scatterplots and gene expression heatmaps. The OS was evaluated using KM survival analysis, and the predictive power of the models was evaluated using receiver operating characteristic (ROC) analysis.

Correlation analysis between *SPDEF* and key prognostic target genes

To elucidate the potential relationship between *SPDEF* expression and its key prognostic target genes, correlation analysis was performed. These four key prognostic genes were derived from risk prognostic models. The correlation between *SPDEF* and each target gene was calculated using the Spearman correlation coefficient.

JASPAR database

The Just Another Spar Promoter Analysis Resource (JASPAR, <http://jaspar.genereg.net/>) database provides a comprehensive collection of transcription factor binding profiles and matrices. It offers valuable insights into potential binding motifs that transcription factors may recognize within gene promoter regions. In this study, the JASPAR database was used to predict the putative *SPDEF*-binding motif within the promoter region of the *S100A16* gene. This information was critical for elucidating the direct interaction between *SPDEF* and the promoter region of *S100A16*.

Cell culture

This study made use of human normal pancreatic ductal cells (HPNE), as well as the PAAD cell lines (BxPC-3, Capan-2, HPAF-II, PANC-1, MIA PaCa-2, and SW1990). The ATCC (Manassas, Virginia, USA) provided all cell lines. Cells were cultured in a humidified incubator at 37°C with 5% CO₂ in a suitable media containing 1% penicillin-streptomycin and 10% fetal bovine serum (FBS). Cells were given either the PI3K inhibitor LY294002 or DMSO as a control in protein studies.

Cell transfection

At a density of 2×10^5 cells per well, PAAD cells were plated in 24-well plates for transient transfection. Plasmids encoding *SPDEF* or *S100A16* were transfected into PAAD cells, allowing for overexpression of these proteins for a designated period. In the control group, cells were transfected with vector plasmids. Knockdown was achieved with specific small interfering RNAs (siRNAs) targeting *SPDEF* (si-SPDEF#1 and si-SPDEF#2) or *S100A16* (si-S100A16#1 and si-S100A16#2). The control group knockdown was done with non-targeting siRNA. The manufacturer's instructions were followed while transfecting cells with Lipofectamine 3000 (Invitrogen, USA). To achieve efficient overexpression or knockdown, cells were further cultured for the optimum amount of time.

Quantitative real-time polymerase chain reaction (qRT-PCR) assay

TRIzol (Thermo Fisher Scientific, USA) was used to extract total RNA from PAAD cells according to the manufacturer's instructions. The PrimeScript RT Reagent Kit (Takara, Japan) was used to perform cDNA. On a StepOnePlus Real-Time PCR System (Applied Biosystems, USA), qRT-PCR was performed using the SYBR Green PCR Master Mix (Applied Biosystems, USA). They were normalized to an internal standard (glyceraldehyde-3-phosphate dehydrogenase, GAPDH). The following are the primer

sequences used for amplification: *SPDEF* forward: 5'-TGTCGCCTTCTACCTCTCCTAC-3', *SPDEF* reverse: 5'-CGATGTCCTTGAGCACTTCGC-3'; *S100A16* forward: 5-

GCTGTCGGACACAGGGAAC-3, *S100A16* reverse: 5-TGATGCCGCCTATCAAGGTC-3. The forward and reverse primers for *GAPDH* were as follows: forward: 5'-CAAGCTCATTTCTGGTATGAC-3', reverse: 5'-CAGTGAGGGTCTCTCTCTTCCT-3'. Using the $2^{-\Delta\Delta CT}$ method, the expression was evaluated.

Western blotting (WB) assay

RIPA lysis buffer (Thermo Fisher Scientific, USA) containing protease and phosphatase inhibitors was used to prepare protein lysates from PAAD cells. The BCA Protein Assay Kit from Thermo Fisher Scientific (USA) was used to calculate the protein concentration. SDS-PAGE was used to separate equal quantities of protein, which was then transferred to PVDF membranes from Millipore (USA). Akt (1:1000, Cell Signaling Technology), p-Akt (1:1000, Cell Signaling Technology), p-GSK3 β (1:1000, Cell Signaling Technology), SPDEF (1:1000, Abcam), S100A16 (1:1000, Abcam), PI3K (1:1000, Abcam), and, finally, GAPDH (1:5000, Cell Signaling Technology), as a control, were used to probe the membranes. After secondary antibody incubation, bands were detected using ECL and captured on a ChemiDoc system.

Cell counting kit-8 (CCK-8) assay

With the help of the CCK-8 assay (Dojindo, Japan), cell viability was evaluated. 96-well plates with a seeding density of 5×10^3 PAAD cells per each well were used. Each well received appropriate treatments before CCK-8 reagent was added. After 0, 24, 48,

72, 96, and 120 h, the absorbance was measured at 450 nm using a microplate reader (Thermo Fisher Scientific, USA).

Flow cytometry analysis

Trypsin-EDTA (Gibco, USA) was used to separate PAAD cells for, and phosphate-buffered saline was used to wash them. According to the manufacturer's recommendations, the cells were stained using fluorescently labeled antibodies specific for SPDEF and S100A16 (Abcam, USA). Data were analyzed using FlowJo software (FlowJo LLC, USA) and flow cytometry was carried out using a flow cytometer (BD Biosciences, USA).

Transwell migration and invasion assay

Twenty-four hours post-transfection, cells were collected and suspended at a density of 5×10^4 cells/well per well. Subsequently, these cells were loaded into the upper chamber of a six-well Transwell insert. To serve as a chemoattractant, full medium was added to the lower chamber. Cells in the top chamber that did not migrate or invade were carefully removed with a cotton swab after 48 hours of incubation at 37°C. A 4% paraformaldehyde was used to fix and DAPI was used to visualize the cell nuclei on the underside of the membrane. Then, using a fluorescent microscope, invading or migrating cells were seen and counted. Images were subsequently captured for documentation.

PCR analysis of chromatin immunoprecipitation (ChIP)

The SimpleChIP Plus Enzymatic Chromatin IP Kit from Cell Signaling Technology and an anti-SPDEF antibody were used to perform ChIP. DNA fragments were enriched and PCR was performed using primers specific for the predicted *SPDEF* binding motif within the *SI00A16* promoter region.

Luciferase activity assay

A luciferase reporter plasmid with either the wild-type (Wt) or mutant (Mut) *SI00A16* promoter sequence was co-transfected into PAAD cells with a plasmid encoding *SPDEF*. The Dual Glo Luciferase Assay System (Promega, Madison, WI) was used in accordance with the manufacturer's instructions to quantify luciferase activity 48 hours after co-transfection. The activity of the *Renilla* luciferase gene was used to normalize firefly luciferase activity.

Statistical analysis

The Statistical Analysis System was used for all analyses, and experiments were triple-replicated. Data were represented as mean \pm SD. Significance ($P < 0.05$) between treatments was ascertained using analysis of variance and Fischer's test at the 95% confidence level. Mortality differences across treatments were evaluated with a chi-square test.

RESULTS

Prognostic significance of *SPDEF* expression in PAAD

The TCGA database yielded 385 upregulated and 605 downregulated DEGs between PAAD samples and normal samples. Further analysis identified five overlapping genes amongst DEGs and ETS family members. To assess the prognostic ramifications of *SPDEF* on essential disease outcomes, namely OS and RFS, we employed the KM method. As depicted in Figures 1C-1D, pancreatic cancer patients with diminished *SPDEF* expression exhibited significantly enhanced OS ($P = 0.0024$) and RFS ($P = 0.011$). This emphasizes the importance of *SPDEF* as a prognostic determinant and its critical role in disease trajectory and patient prognosis. Subsequent expression evaluations unveiled a marked *SPDEF* increase within PAAD tumor specimens, implying its proto-oncogenic role (Figure 1E). Further assessment of *SPDEF* expression and PAAD tumor stages, resulted in a pronounced *SPDEF* expression in stage 2 tumours (Figure 1F). An in-depth appraisal of both M-stage and N-stage categories corroborated the sustained elevation of *SPDEF* in PAAD tumor specimens, with its expression independent of M-stage and N-stage distinctions (Figures 1G-1H). For *in vitro* evaluations, our selection encompassed HPNE and a spectrum of PAAD cells. Through qRT-PCR and WB analytical methodologies, we ascertained a significant upregulation of *SPDEF* in pancreatic cancer cells, predominantly within PANC-1 and MIA PaCa-2 lines (Figures 1I-1J), designating them for further experimental exploration.

Effects of *SPDEF* regulation on the phenotype of PAAD cells

Utilizing qRT-PCR and WB analyses, we studied the effects of *SPDEF* manipulation on MIA PaCa-2 and PANC-1 cells (Figures 2A-2D). We observed that overexpression of *SPDEF* significantly increased both mRNA and protein levels. Conversely, *SPDEF* knockdown led to substantial reductions in these levels, with the most pronounced decrease seen in si-*SPDEF*#1. To understand the functional implications of these alterations, we employed the CCK-8 assay. Cells with enhanced *SPDEF* expression showed notable proliferation, as indicated by increased absorbance values. However, cells with reduced *SPDEF* expression displayed diminished proliferation, evidenced by decreased absorbance values (Figures 2E-2F). Collectively, our data emphasizes the pivotal role *SPDEF* plays in influencing the behavior of PAAD cells.

***SPDEF* promotes PAAD cell invasion and metastasis and inhibits apoptosis in vitro**

Flow cytometry provides a compelling method to study cellular apoptosis. Our results revealed that enhanced *SPDEF* expression leads to a decline in apoptosis (Figures 3A-3D). Conversely, cells with downregulated *SPDEF* exhibited pronounced apoptotic activity. Further diving into the effects of *SPDEF* on PAAD cell dynamics, we employed the Transwell assay to gauge cell migration and invasion capabilities. Cells enriched with *SPDEF* exhibited pronounced migratory and invasive properties. In contrast, *SPDEF*-inhibited cells demonstrated significantly diminished capacities in both assays (Figures 3E-3J). Together, these insights underscore the instrumental role of *SPDEF* in shaping the behavior of PAAD cells.

SPDEF target gene identification and prognostic value analysis

Identifying target genes of SPDEF holds a promise for advancing our understanding of its role in PAAD. To discern these potential targets, we utilised the hTFtarget database. From the intersection of the predicted targets and upregulated DEGs, a subset of 30 candidate genes emerged. LASSO regression analysis, with an optimal λ_{\min} value pinpointed at 0.0722 (Figures 4A and 4B), further distilled this list to four paramount genes: *S100A16*, *MMP28*, *ECT2*, and *MYEOV* (Figure 4C). Furthermore, KM survival analysis revealed that samples with a higher risk profile have a decreased OS probability (Figure 4D). Additionally, ROC curve analysis indicated that the risk model possessed good prognostic predictive capabilities, with AUC values exceeding 0.7 at the 1-, 3-, and 5-year marks (Figure 4E).

SPDEF activates transcription of *S100A16*

We commenced with a correlation analysis involving SPDEF and its four putative targets: *S100A16*, *MMP28*, *ECT2*, and *MYEOV* (Figure 5A). *S100A16* emerged with the most potent correlation to SPDEF, prompting us to investigate further into its relationship. Our experimental observations indicated that elevating *S100A16* levels in PAAD cells led to a surge in SPDEF expression (Figures 5B and 5C). Conversely, curbing *S100A16* resulted in diminished SPDEF levels. We then employed JASPAR to predict potential SPDEF-binding sites within the *S100A16* promoter, identifying several candidates (Figure 5D). To authenticate a direct interaction between SPDEF and the *S100A16* promoter, ChIP-PCR was utilized. The analysis validated SPDEF

enrichment on the *S100A16* promoter, with sequences from the binding region being amplified when DNA was precipitated with Flag-tagged SPDEF (Figures 5E-5F). To further investigate SPDEF's transcriptional influence on *S100A16*, we introduced both the wild-type (Wt) and binding site mutants (Mut) of the *S100A16* promoter into the pGL4.20 vector. Post-transfection into PAAD cells, luciferase reporter assays demonstrated an augmentation in *S100A16* promoter activity upon SPDEF expression. Notably, this amplification was nullified when the SPDEF binding site underwent mutation (Figures 5G-5H).

S100A16 mediates SPDEF-induced proliferation, migration, and invasion of PAAD cells

We conducted a series of experiments to evaluate the interplay between SPDEF and S100A16 and the subsequent impact on PAAD cell behaviors. Figures 6A-6D showcase our findings using qRT-PCR and WB analyses, revealing a stark reduction in S100A16 expression upon its knockdown in PAAD cells. Conversely, amplifying S100A16 levels resulted in its increased expression. Subsequent functional analyses elucidated the implications of these modulations. CCK-8 assays depicted that the proliferation of PAAD cells surged with heightened SPDEF expression. Remarkably, concomitant knockdown of *S100A16* in SPDEF-overexpressing cells led to a pronounced reduction in proliferation, even surpassing the drop observed in the control group (Figures 6E-6F). To further decipher the role of S100A16 in SPDEF-mediated cellular behaviors, we carried out migration and invasion assays. Figures 6G-6L depict a noticeable

enhancement in the migratory and invasive potential of PAAD cells under SPDEF overexpression. Yet, an intriguing observation was made: when SPDEF-overexpressing cells underwent simultaneous *S100A16* knockdown, their migration and invasion capabilities reduced dramatically, even plunging below control group levels.

SPDEF promotes PAAD progression by transcriptionally upregulating *S100A16* and activating the PI3K/AKT signaling pathway

To explore the interplay between the PI3K/AKT/p-GSK3 β signaling cascade and *S100A16* in cellular dynamics, we set up a comprehensive experimental approach using PAAD cells (Figures 7A-7F). Our initial approach involved the transfection of cells with SPDEF overexpression individually, in tandem with LY294002 (a PI3K antagonist at 10 μ M), or following *S100A16* knockdown at 10 μ g/mL. Subsequent WB analyses highlighted that SPDEF increase resulted in heightened levels of p-Akt, and p-GSK3 β . Intriguingly, combining SPDEF overexpression with LY294002 led to a decline in p-Akt, and p-GSK3 β levels, albeit these levels remained above control values. On the other end of the spectrum, integrating SPDEF overexpression with *S100A16* attenuation witnessed a drop in p-Akt, and p-GSK3 β expressions. Notably, significant alterations, as gauged by WB, were predominantly seen in p-Akt and p-GSK3 β . Collectively, our data highlights the pivotal role that *S100A16* plays in orchestrating the influence of SPDEF on the PI3K/AKT signaling pathway, thereby shedding light on intricate molecular dynamics governing PAAD cell behavior.

DISCUSSION

In this study, we delineate the pivotal influence of *SPDEF* gene on cancer progression, particularly in the context of the PI3K/AKT pathway. Although previous studies have implicated *SPDEF*'s role in various tumors, its unique role in specific cancer manifestations remains unclear. Therefore, we deeply investigated the multifaceted functions and mechanisms of *SPDEF* in PAAD. Our data highlighted the integral role of *SPDEF* in the complex progression of PAAD, primarily driven by activation of the PI3K/AKT signaling cascade. Although the role of *SPDEF* and the PI3K/AKT pathway in PAAD has already been established in cancer, the symbiotic relationship between *SPDEF* and the PI3K/AKT pathway remains a pathway of interest. Our findings bridge this knowledge gap, offering invaluable insights into the molecular intricacies propelling PAAD progression.

Commencing our exploration, a bioinformatics-driven approach was deployed, enabling the identification of *SPDEF* as a crucial regulator in the intricate tapestry of pancreatic cancer dynamics. *SPDEF* plays pivotal roles in myriad biological functions (20-22). While its association with oncogenesis is established, the nuances of its involvement are variegated, with manifestations differing across cancer types. For instance, in the realm of breast cancer, Ye et al. spotlighted *SPDEF*'s paradoxical nature, demonstrating both its oncogenic and tumor-suppressive propensities (23). Divergently, in colorectal cancers, Lo et al. delineated how *SPDEF* induces cellular quiescence, orchestrating this through its regulation of β -catenin transcriptional targets (22). These

seemingly contradictory roles highlight the depth and breadth of SPDEF's influence in cancer biology, underscoring its prominence as a key to a potential treatment. In our findings, a negative correlation was found between the expression of SPDEF and disease prognosis. Furthermore, SPDEF expression was upregulated in PAAD tumor specimens, especially in stage 2 tumors. This is consistent with the sequential expression pattern in M and N stages, suggesting its role as a proto-oncogene. Moreover, in vitro functional assessment further revealed the extensive role of SPDEF in the regulation of PAAD cells. Overexpression of SPDEF leads to changes in cell behavior, promoting proliferation, migration, and invasion while inhibiting apoptosis. In conclusion, our study clarifies the multifaceted role of SPDEF in PAAD and provides new insights into its potential as a diagnostic and therapeutic target.

In our comprehensive exploration, we meticulously identified *S100A16* as a target gene of SPDEF through a strategic fusion of bioinformatics tools, regression analysis, and experimental validation. *S100A16*, part of the expansive S100A family, has begun carving out its niche in oncology, portraying a tale of multifaceted roles within tumorigenesis (24, 25). Intriguingly, research by Li et al. highlighted an upregulated expression of *S100A16* and its related family members in PDAC tissues when juxtaposed with their normal counterparts (26). This upsurge in expression, which is inversely proportional to promoter methylation, strikingly correlates with a decline in the survival rates of PDAC patients, signaling its potential as a prognostic biomarker. Notably, the elevated S100A16 expression in PAAD is intriguingly counteracted by its

negative association with immune activity and infiltration, particularly with CD8⁺ T cells, shedding light on its dual capacity as a prognostic marker and a therapeutic target for immune interventions. Adding more layers to this intricate relationship, Li et al. discovered that S100A16 promotes PDAC metastasis by activating the STAT3 signaling cascade, inducing epithelial-to-mesenchymal transition (24). This revelation underlines the possibility that attenuating S100A16 can enhance the anti-tumor efficacy of agents like gemcitabine, branding it as a prospective target in PDAC treatment regimens. Another study delineated an overexpression of S100A16 in PDAC, pinpointing its role in advancing the disease through the FGF19-mediated AKT and ERK1/2 signaling pathways, further supporting its candidacy as a therapeutic target (27). From our results, *S100A16* was determined to be the key target gene of SPDEF in PAAD. When S100A16 levels change, SPDEF expression adjusts accordingly, showing a direct interrelationship between them. Moreover, S100A16 low expression effectively counteracted the promotion effect of SPDEF overexpression on PAAD cell growth.

The PI3K/AKT signaling pathway is recognized as the primary regulatory network in the investigation of the intricate mechanisms behind pancreatic cancer and is intimately related to several biological functions (28-30). The PI3K/AKT signaling pathway is essential for maintaining healthy cell function, but it also plays a crucial role in the development of cancer (31). For example, reports indicate that when the PI3K/AKT pathway is abnormally activated, it leads to unlimited proliferation of pancreatic cancer cells and apoptosis inhibition, thus providing support for tumor growth and metastasis

(32). Another study discovered that some medications that block the PI3K/AKT pathway are capable of stopping pancreatic cancer cells from migrating and invading, showing the critical role of this pathway in pancreatic cancer (33). Based on the above background, we conducted a comprehensive investigation into the interplay of the PI3K/AKT/p-GSK3 β signaling pathway with S100A16 in pancreatic cancer cells. Our experimental results demonstrated that when SPDEF was overexpressed, the levels of p-Akt and p-GSK3 β greatly increased. Combined with LY294002, the antagonist of PI3K, or *S100A16* knockdown, these expression levels were reduced. These results emphasize the pivotal role of S100A16 in modulating the impact of SPDEF on the PI3K/AKT signaling pathway. Overall, our findings provide fresh light on the molecular basis of pancreatic cancer by highlighting the significant regulatory role of S100A16 on the PI3K/AKT signaling pathway.

In summary, our comprehensive investigation underscores the profound implications of SPDEF and its target gene, *S100A16*, in the progression and dynamics of PAAD cells. SPDEF emerged as a pivotal determinant, profoundly influencing cell proliferation, migration, and invasion. Notably, its transcriptional upregulation of *S100A16* unraveled a significant nexus in shaping PAAD cell behavior. Moreover, the involvement of the PI3K/AKT signaling pathway further elucidates the molecular complexity underpinning the translational effects promoted by SPDEF via *S100A16*. These findings illuminate potential therapeutic avenues, emphasising the need to further explore these molecular dynamics for effective PAAD intervention.

ACKNOWLEDGEMENTS

The authors thank all patients involved in this study.

REFERENCES

1. Kaschwich M, Peters F, Hischke S, Rieß HC, Gansel M, Marschall U, et al. Long-term incidence of cancer after index treatment for symptomatic peripheral arterial disease—a health insurance claims data analysis. *Vasa*. 2020.
2. Yu X, Zhang Q, Gao F, Zhang M, Zheng Q, He Y, et al. Predictive value of m5C regulatory gene expression in pancreatic adenocarcinoma. *Scientific Reports*. 2021;11(1):17529.
3. Zhou Z, Zhang Y, Li J, Weng S, Li J, Chen S, et al. Crosstalk between regulated cell death and immunity in redox dyshomeostasis for pancreatic cancer. *Cellular Signalling*. 2023:110774.
4. Zhao G, Wang C, Jiao J, Zhang W, Yang H. The novel subclusters based on cancer-associated fibroblast for pancreatic adenocarcinoma. *Frontiers in Oncology*. 2022;12:1045477.
5. Biederstädt A, Hassan Z, Schneeweis C, Schick M, Schneider L, Muckenhuber A, et al. SUMO pathway inhibition targets an aggressive pancreatic cancer subtype. *Gut*. 2020;69(8):1472-82.
6. Li X, Zhang X, Lin X, Cai L, Wang Y, Chang Z. Classification and prognosis analysis of pancreatic cancer based on DNA methylation profile and clinical information. *Genes*. 2022;13(10):1913.
7. Wang X, Li L, Yang Y, Fan L, Ma Y, Mao F. Reveal the heterogeneity in the tumor microenvironment of pancreatic cancer and analyze the differences in prognosis and immunotherapy responses of distinct immune subtypes. *Frontiers in Oncology*.

2022;12:832715.

8. Teng Y, Fan Y, Ma J, Lu W, Liu N, Chen Y, et al. The PI3K/Akt pathway: emerging roles in skin homeostasis and a group of non-malignant skin disorders. *Cells*. 2021;10(5):1219.
9. Slattery ML, Mullany LE, Sakoda LC, Wolff RK, Stevens JR, Samowitz WS, et al. The PI3K/AKT signaling pathway: associations of miRNAs with dysregulated gene expression in colorectal cancer. *Molecular carcinogenesis*. 2018;57(2):243-61.
10. Razaghi A, Heimann K, Schaeffer PM, Gibson SB. Negative regulators of cell death pathways in cancer: perspective on biomarkers and targeted therapies. *Apoptosis*. 2018;23:93-112.
11. Pungsrinont T, Kallenbach J, Baniahmad A. Role of PI3K-AKT-mTOR pathway as a pro-survival signaling and resistance-mediating mechanism to therapy of prostate cancer. *International journal of molecular sciences*. 2021;22(20):11088.
12. Ebrahimi S, Hosseini M, Shahidsales S, Maftouh M, A Ferns G, Ghayour-Mobarhan M, et al. Targeting the Akt/PI3K signaling pathway as a potential therapeutic strategy for the treatment of pancreatic cancer. *Current medicinal chemistry*. 2017;24(13):1321-31.
13. Rahmani F, Ziaemehr A, Shahidsales S, Gharib M, Khazaei M, Ferns GA, et al. Role of regulatory miRNAs of the PI3K/AKT/mTOR signaling in the pathogenesis of hepatocellular carcinoma. *Journal of cellular physiology*. 2020;235(5):4146-52.
14. Sanaei M-J, Razi S, Pourbagheri-Sigaroodi A, Bashash D. The PI3K/Akt/mTOR pathway in lung cancer; oncogenic alterations, therapeutic opportunities, challenges,

and a glance at the application of nanoparticles. *Translational Oncology*. 2022;18:101364.

15. Zhang H, Pan Y-z, Cheung M, Cao M, Yu C, Chen L, et al. LAMB3 mediates apoptotic, proliferative, invasive, and metastatic behaviors in pancreatic cancer by regulating the PI3K/Akt signaling pathway. *Cell Death & Disease*. 2019;10(3):230.

16. Stanciu S, Ionita-Radu F, Stefani C, Miricescu D, Stanescu-Spinu I-I, Greabu M, et al. Targeting PI3K/AKT/mTOR signaling pathway in pancreatic cancer: from molecular to clinical aspects. *International Journal of Molecular Sciences*. 2022;23(17):10132.

17. Li N, Yang F, Liu D-Y, Guo J-T, Ge N, Sun S-Y. Scoparone inhibits pancreatic cancer through PI3K/Akt signaling pathway. *World journal of gastrointestinal oncology*. 2021;13(9):1164.

18. Sun X, Wang T, Zhang C, Ning K, Guan ZR, Chen SX, et al. S100A16 is a prognostic marker for colorectal cancer. *Journal of surgical oncology*. 2018;117(2):275-83.

19. Sun H, Zhao A, Li M, Dong H, Sun Y, Zhang X, et al. Interaction of calcium binding protein S100A16 with myosin-9 promotes cytoskeleton reorganization in renal tubulointerstitial fibrosis. *Cell Death & Disease*. 2020;11(2):146.

20. Wu J, Qin W, Wang Y, Sadik A, Liu J, Wang Y, et al. SPDEF is overexpressed in gastric cancer and triggers cell proliferation by forming a positive regulation loop with FoxM1. *Journal of Cellular Biochemistry*. 2018;119(11):9042-54.

21. Meiners J, Schulz K, Möller K, Höflmayer D, Burdelski C, Hube-Magg C, et al.

Upregulation of SPDEF is associated with poor prognosis in prostate cancer. *Oncology Letters*. 2019;18(5):5107-18.

22. Lo Y-H, Noah TK, Chen M-S, Zou W, Borrás E, Vilar E, et al. SPDEF induces quiescence of colorectal cancer cells by changing the transcriptional targets of β -catenin. *Gastroenterology*. 2017;153(1):205-18. e8.

23. Ye T, Feng J, Wan X, Xie D, Liu J. Double agent: SPDEF gene with both oncogenic and tumor-suppressor functions in breast cancer. *Cancer management and research*. 2020:3891-902.

24. Li T, Ren T, Huang C, Li Y, Yang P, Che G, et al. S100A16 induces epithelial-mesenchymal transition in human PDAC cells and is a new therapeutic target for pancreatic cancer treatment that synergizes with gemcitabine. *Biochemical pharmacology*. 2021;189:114396.

25. Ou S, Liao Y, Shi J, Tang J, Ye Y, Wu F, et al. S100A16 suppresses the proliferation, migration and invasion of colorectal cancer cells in part via the JNK/p38 MAPK pathway. *Molecular Medicine Reports*. 2021;23(2):1-.

26. Li H-B, Wang J-L, Jin X-D, Zhao L, Ye H-L, Kuang Y-b, et al. Comprehensive analysis of the transcriptional expressions and prognostic value of S100A family in pancreatic ductal adenocarcinoma. *BMC cancer*. 2021;21(1):1-18.

27. Fang D, Zhang C, Xu P, Liu Y, Mo X, Sun Q, et al. S100A16 promotes metastasis and progression of pancreatic cancer through FGF19-mediated AKT and ERK1/2 pathways. *Cell biology and toxicology*. 2021:1-17.

28. Xue R, Meng Q, Lu D, Liu X, Wang Y, Hao J. Mitofusin2 induces cell autophagy

of pancreatic cancer through inhibiting the PI3K/Akt/mTOR signaling pathway.

Oxidative Medicine and Cellular Longevity. 2018;2018.

29. Wang L, Zhang B, Zheng W, Kang M, Chen Q, Qin W, et al. Exosomes derived from pancreatic cancer cells induce insulin resistance in C2C12 myotube cells through the PI3K/Akt/FoxO1 pathway. *Scientific reports*. 2017;7(1):5384.

30. Xu R, Song J, Ruze R, Chen Y, Yin X, Wang C, et al. SQLE promotes pancreatic cancer growth by attenuating ER stress and activating lipid rafts-regulated Src/PI3K/Akt signaling pathway. *Cell Death & Disease*. 2023;14(8):497.

31. Sun K, Luo J, Guo J, Yao X, Jing X, Guo F. The PI3K/AKT/mTOR signaling pathway in osteoarthritis: a narrative review. *Osteoarthritis and cartilage*. 2020;28(4):400-9.

32. Zou Z, Tao T, Li H, Zhu X. mTOR signaling pathway and mTOR inhibitors in cancer: progress and challenges. *Cell & Bioscience*. 2020;10(1):1-11.

33. Li W, Jiang Z, Xiao X, Wang Z, Wu Z, Ma Q, et al. Curcumin inhibits superoxide dismutase-induced epithelial-to-mesenchymal transition via the PI3K/Akt/NF- κ B pathway in pancreatic cancer cells. *International journal of oncology*. 2018;52(5):1593-602.

FIGURE LEGENDS

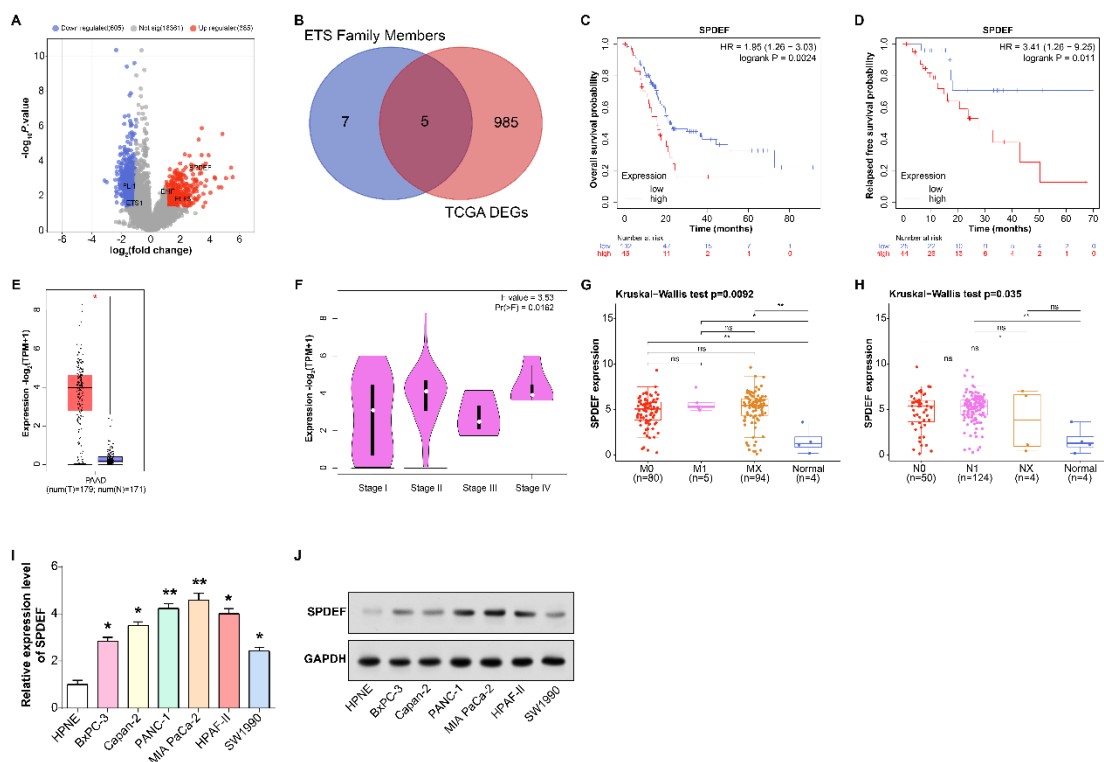


Figure 1. Expression and prognostic analysis of *SPDEF* in pancreatic PAAD.

(A) Analysis of DEGs in PAAD samples and normal control samples in the TCGA database. Red scattered points represent upregulated DEGs, and blue scattered points represent downregulated DEGs. (B) Venn diagram, analysis of overlapping genes between TCGA-DEGs and ETS family members. (C-D) The impact of differential expression of *SPDEF* on OS prognosis and RFS prognosis in PAAD patients. Blue represents low expression samples, red represents high expression samples. (E) Box plot, validation of *SPDEF* expression in PAAD tumor samples in the GEPIA database. (F-H) Expression of *SPDEF* in different stage subgroups in the GEPIA database, including M stage and N stage. (I-J) qRT-PCR and western blot detected the expression of *SPDEF* in control cells and 6 PAAD cell lines. * $P<0.05$. ** $P<0.01$. ns: not significant.

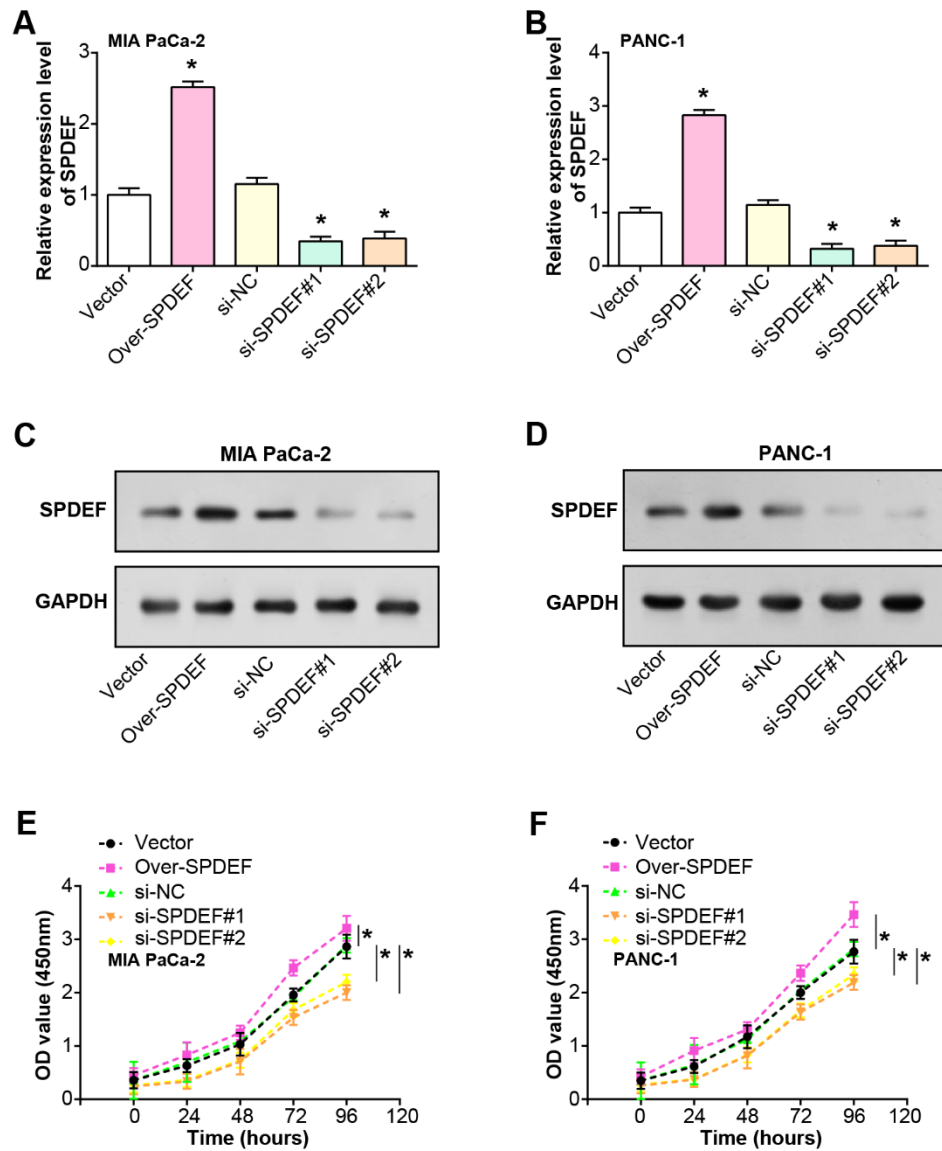


Figure 2. Regulation of PAAD cell phenotype by overexpression and knockdown of *SPDEF*. (A-D) qRT-PCR and western blot analyses were used to investigate the effect of *SPDEF* regulation on the phenotype of PAAD cells. (E-F) Functional analysis using the CCK-8 assay to assess cell proliferation in response to *SPDEF* modulation. * $P < 0.05$. ** $P < 0.01$.

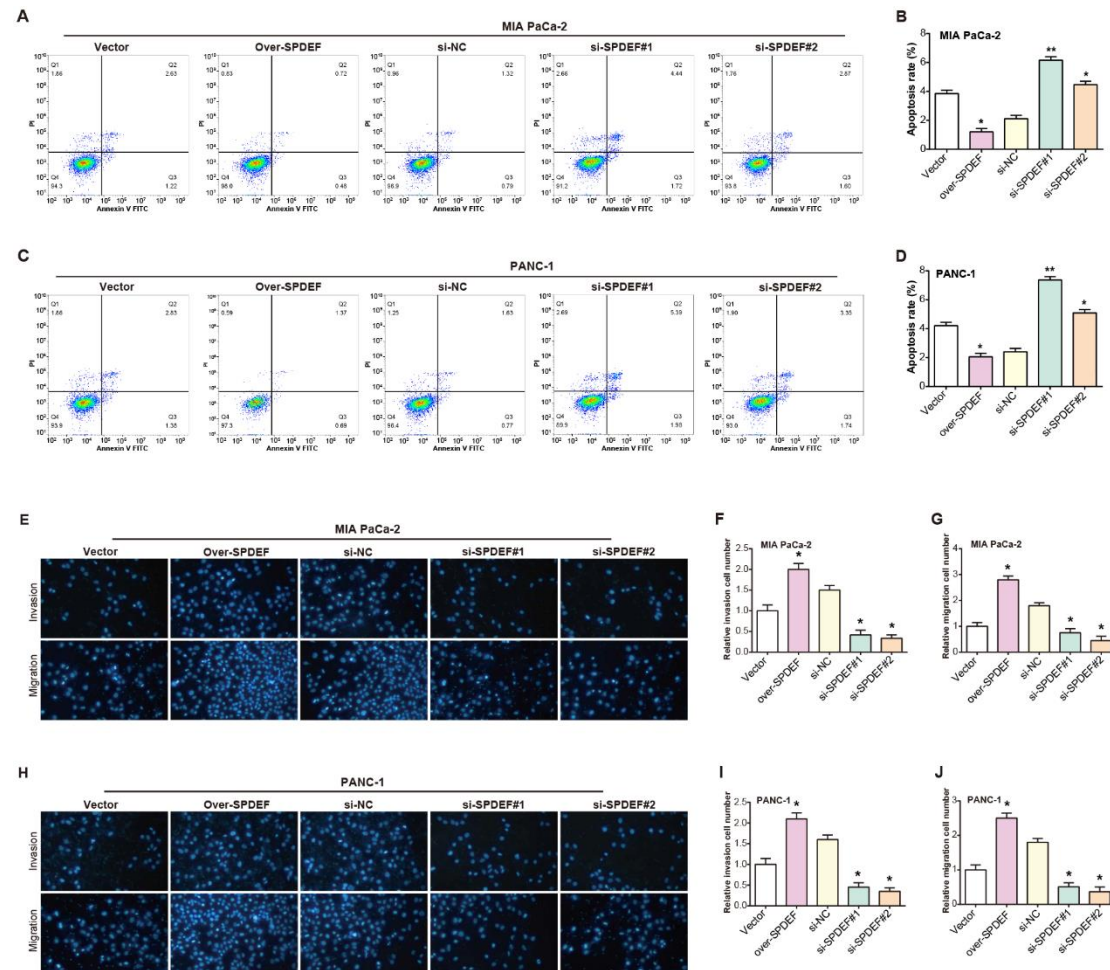
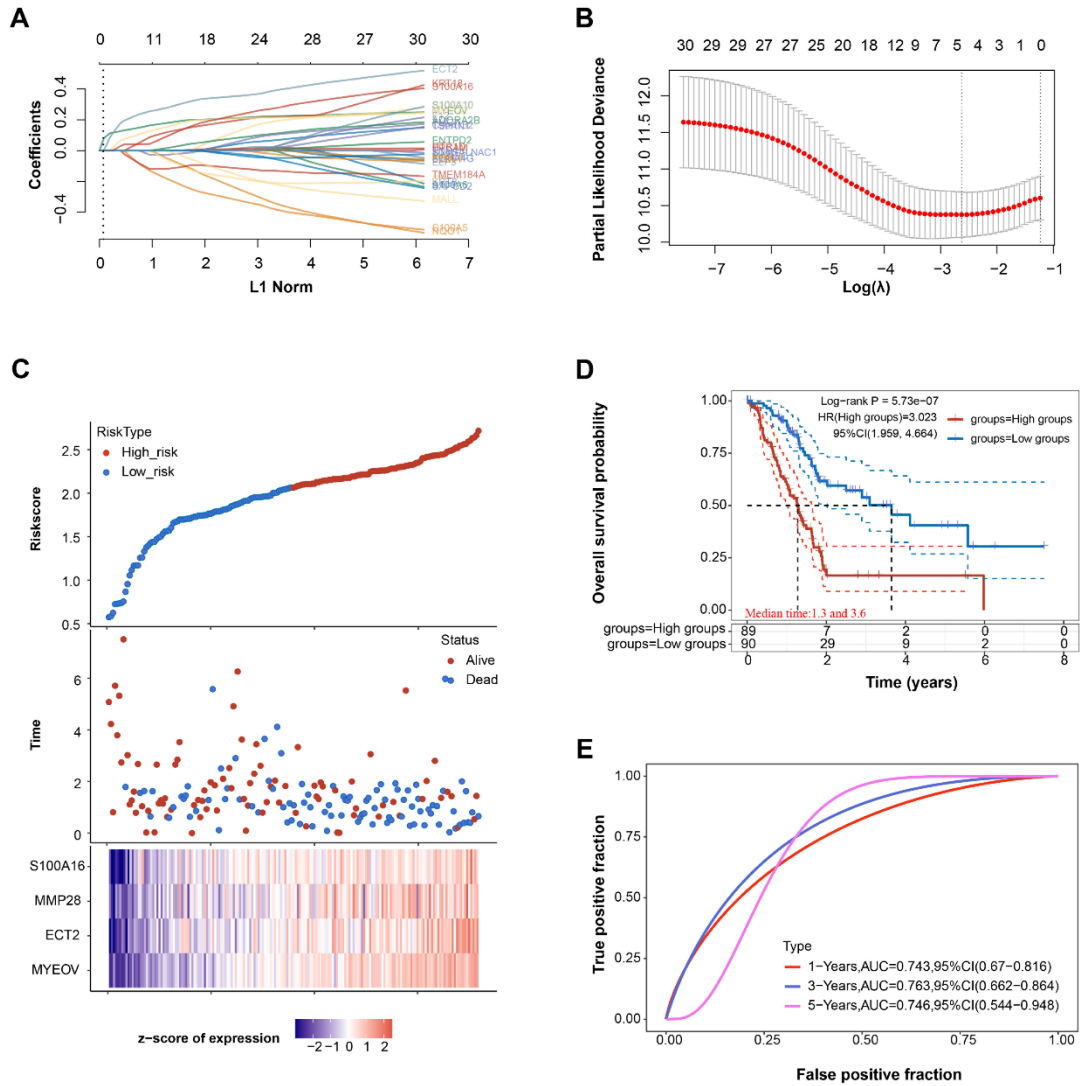
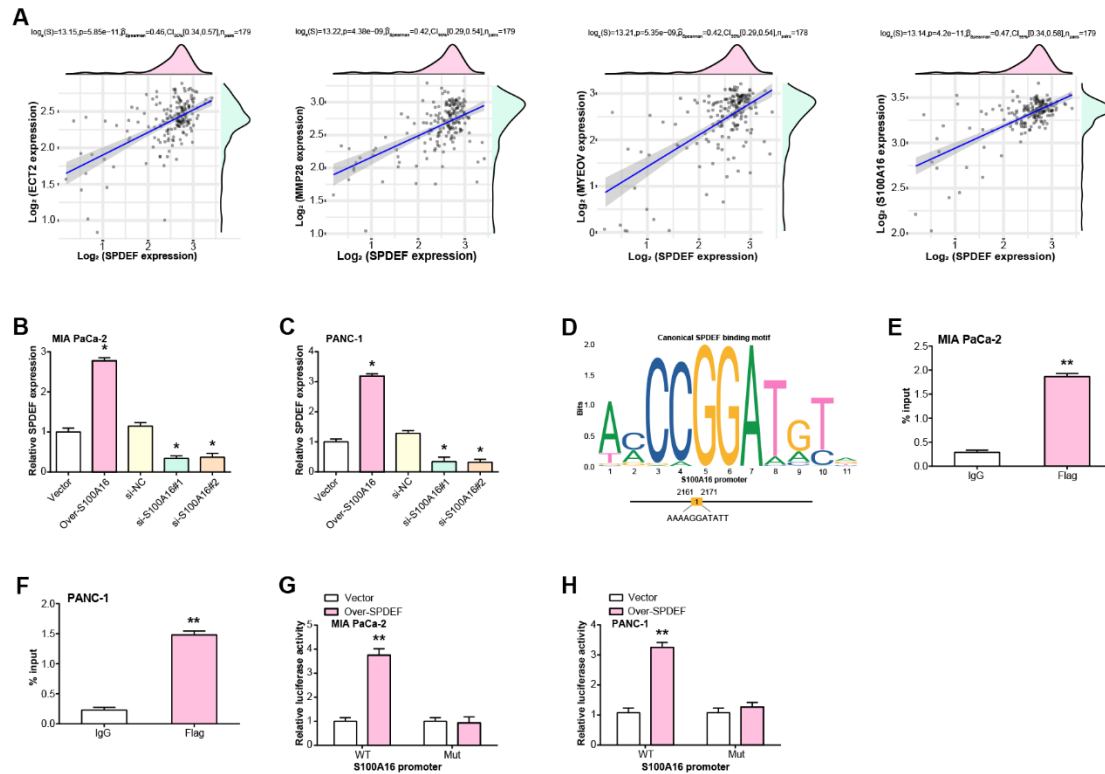


Figure 3. Differential expression of *SPDEF* regulates PAAD cell apoptosis, migration and invasion. (A-D) The effects of *SPDEF* overexpression or knockdown on apoptosis in vitro were evaluated by flow cytometry analysis. (E-J) Transwell experiment to study the effects of *SPDEF* overexpression or knockdown on cell migration and invasion. ** $P < 0.01$.



Figures 4. SPDEF target gene identification and prognostic value analysis in PAAD. (A) LASSO coefficient profiles of the 30 candidate genes. The vertical line is drawn at the value chosen by 10-fold cross-validation. (B) Partial likelihood deviance plot versus $\log(\lambda)$. The dotted vertical lines represent the optimal values using the minimum criteria and the 1 standard error of the minimum criteria. (C) Display of the four significant genes (*S100A16*, *MMP28*, *ECT2*, and *MYEOV*) filtered by LASSO regression, along with their risk scores and survival status. The heatmap below shows the z-score of expression for these genes. (D) Kaplan-Meier survival curves for patients grouped by high and low risk. The number of patients at risk in each group is displayed below the survival curve. (E) ROC curve analysis for the prognostic risk model at 1-, 3-, and 5-year survival periods. AUC values for each interval are provided in the legend.



Figures 5. SPDEF activates the transcription of *S100A16* in PAAD cells.

(A) Correlation analysis between SPDEF expression and its four putative targets (*S100A16*, *MMP28*, *ECT2*, and *MYEOV*). The scatter plots show the correlation coefficient (R) and the P-value. (B-C) Expression levels of SPDEF after upregulation or knockdown of *S100A16* in MIA PaCa-2 (B) and PANC-1 (C) cells. Bars indicate relative SPDEF expression. (D) The canonical SPDEF binding motif and predicted SPDEF-binding sites within the *S100A16* promoter region. (E-F) ChIP-PCR validation of SPDEF binding to the *S100A16* promoter. The histogram displays enrichment levels of the *S100A16* promoter region in Flag-tagged SPDEF precipitated DNA in MIA PaCa-2 (E) and PANC-1 (F) cells. (G-H) Luciferase reporter assays showing the transcriptional activity of the wild-type and mutated *S100A16* promoter upon SPDEF expression in MIA PaCa-2 (G) and PANC-1 (H) cells. Bars represent relative luciferase activity.

* $P < 0.05$, ** $P < 0.01$.

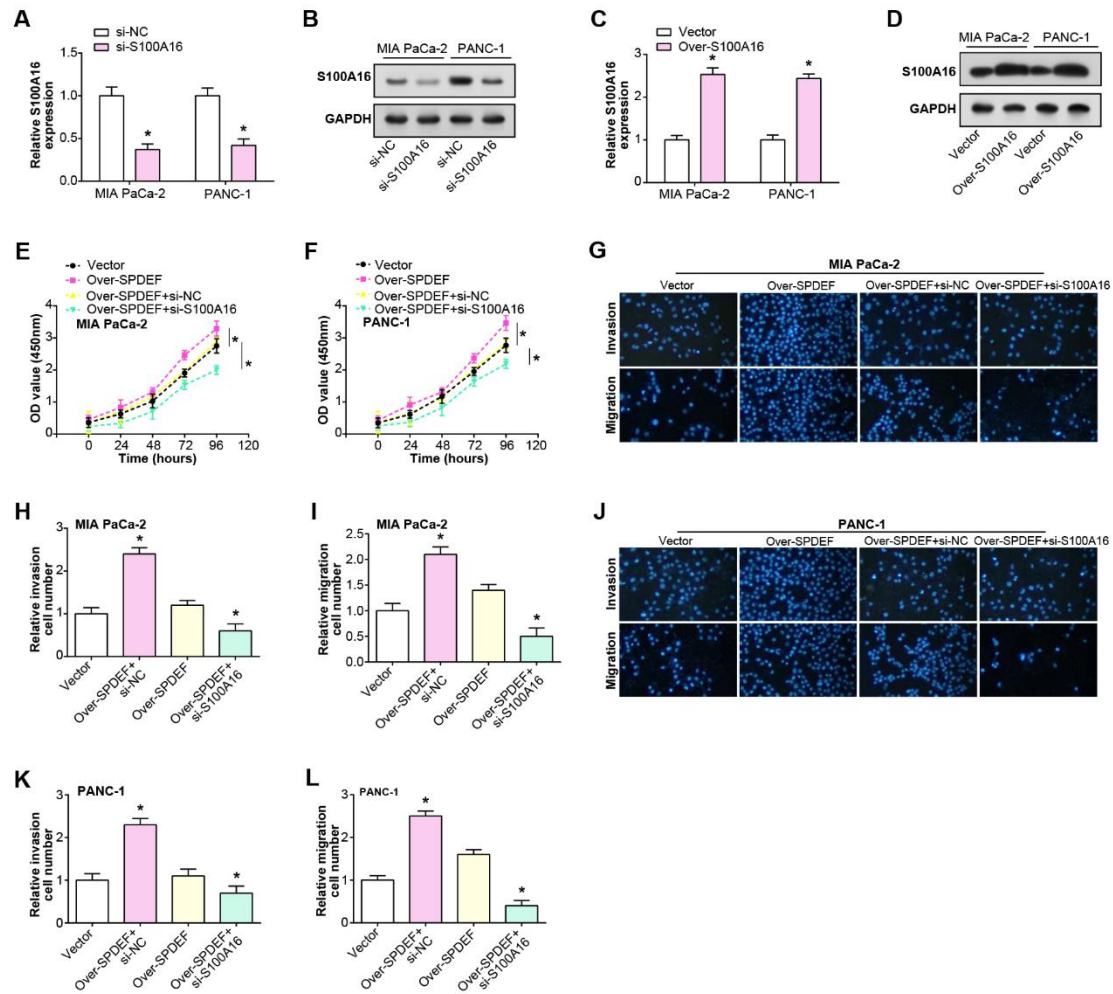


Figure 6. S100A16 coordinates SPDEF-induced proliferation, migration and invasion of pancreatic cancer cells. (A-D) Expression analysis of *S100A16* by qRT-PCR and western blot after *S100A16* knockdown and *S00A16* overexpression in PAAD cells. (E-F) CCK-8 assay to determine the regulation of cell proliferation by *S100A16* knockdown and overexpression of SPDEF. (G-L) Transwell assay to evaluate the effects of *S100A16* knockdown and overexpression of SPDEF on cell migration and invasion abilities. * $P < 0.05$.

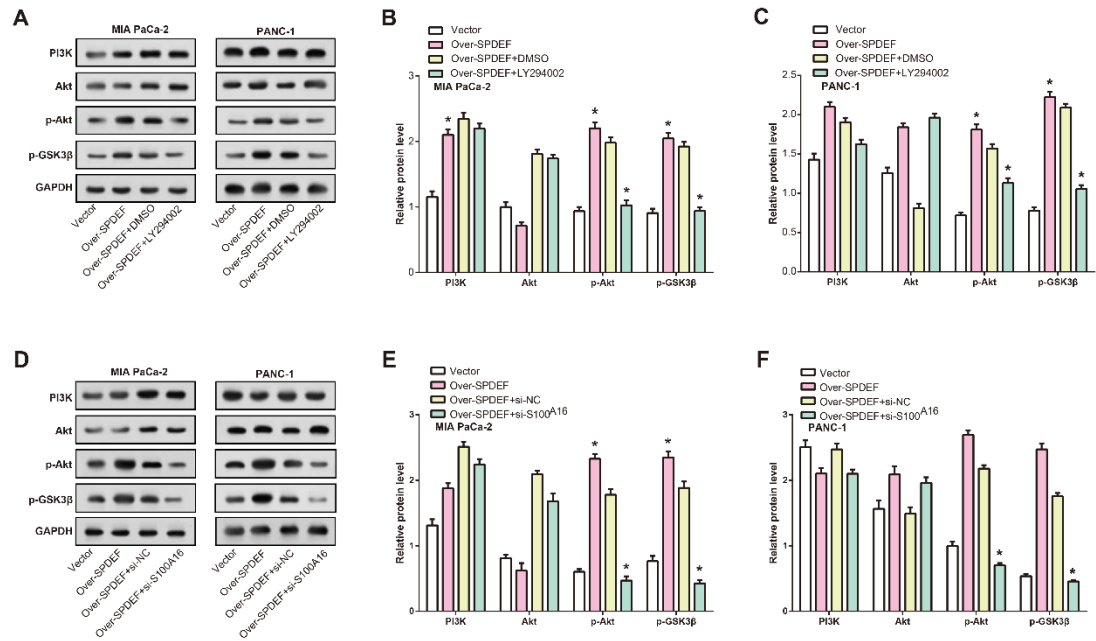


Figure 7. SPDEF modulates PI3K/AKT/p-GSK3β signaling cascade in PAAD cells. (A-B) Western blot analysis representing the impact of SPDEF overexpression, either alone or in conjunction with LY294002 treatment, on the expression levels of PI3K, Akt, p-Akt, and p-GSK3β in MIA PaCa-2 and PANC-1 cells. GAPDH was employed as a loading control. (C) Quantification of protein levels in MIA PaCa-2 and PANC-1 cells treated as described in (A-B). (D-E) Western blot analysis showcasing the effect of SPDEF overexpression either individually or following *S100A16* knockdown on the expression of PI3K, Akt, p-Akt, and p-GSK3β in MIA PaCa-2 and PANC-1 cells. GAPDH served as a loading control. (F) Quantitative assessment of protein expressions in MIA PaCa-2 and PANC-1 cells treated as mentioned in (D-E). * $P < 0.05$.

SUPPLEMENTAL DATA

Supplementary Table 1. List of thirty SPDEF target genes

Gene
<i>C9orf152</i>
<i>TMEM184A</i>
<i>F2RL1</i>
<i>ID1</i>
<i>SAPCD2</i>
<i>KRT8</i>
<i>ENTPD2</i>
<i>MALL</i>
<i>S100A16</i>
<i>EPCAM</i>
<i>ECT2</i>
<i>MYEOV</i>
<i>KRT18</i>
<i>ADORA2B</i>
<i>HTR1D</i>
<i>MANSC1</i>
<i>TMC7</i>
<i>ST6GALNAC1</i>
<i>S100A5</i>
<i>ELF3</i>
<i>S100A6</i>
<i>SH3RF2</i>
<i>MMP28</i>
<i>NQO1</i>
<i>TNS4</i>
<i>SEMA4G</i>
<i>S100A10</i>
<i>TSPAN1</i>
<i>F12</i>
<i>FOSL1</i>